International Journal of Creative and Open Research in Engineering and Management
ISSN: 3108-1754 (Online)
Volume 02 Issue 09 September-2026 | Impact Factor: 3.5

"Structural Evolution, Surface Morphology and Vibrational Characteristics of CuO (Cupric Oxide) Composite Oxides"

Manjula V T [1] Nagajyoti[2]

.

1. Dept. Of Physics Government First Grade College Jewargi
2. Department of physics, government college (Autonomus), Kalaburagi-585105,hiremathnagajyoti79@gmail.com

Corresponding author: Dr. Nagajyoti (email: hiremathnagajyoti79@gmail.com)

How to Cite this Article:

T, M. V. & Nagajyoti, (2026). Structural Evolution, Surface Morphology and Vibrational Characteristics of CuO (Cupric Oxide) Composite Oxides. International Journal of Creative and Open Research in Engineering and Management, 02(9), 1-9. https://doi.org/10.55041/ijcope.v2i9.018

https://doi.org/10.55041/ijcope.v2i9.018

Abstract

Insitu polymerization technique was adopted by preparation of pani-anilline and compopsite pani-aniline (PANI-CuO) the ammonium Persulphate as a oxidizing agent. CuO (cupric oxide) composite oxides were examined to know their structurally, morphologically, and vibrationally features. X-ray diffraction (XRD) investigation was used to estimate the crystallinity, phase construction, and structural progress of the complexes. SEM (scanning electron microscopy) investigates the size of the particle and morphological surface and also particle distributions. FTIR determines the bonding structures, mode of the vibrational and shows the functional group. . The results demonstrate that the CuO composite oxides exhibit distinct structural and morphological features suitable for advanced functional applications.

Keywords

PANI, CuO, APS, HCL XRD, SEM, FTIR.

Introduction

Polymers are an important class of materials that have attracted considerable attention because of their low density, flexibility, chemical stability, low cost, ease of processing, and versatile properties. They are widely used in electronics, energy storage, sensors, coatings, biomedical devices, and environmental applications. Among functional polymers, conducting polymers are particularly important because they combine the flexibility and processability of polymers with electrical conductivity. Polyaniline (PANI) is one of the most extensively investigated conducting polymers because of its simple synthesis, low cost, good environmental stability, tunable electrical conductivity, and reversible redox properties [1–2]. PANI exists in different oxidation states, of which the emeraldine form is particularly important because of its relatively high electrical conductivity after protonic-acid doping. PANI can be synthesized by chemical oxidative polymerization of aniline using an oxidizing agent such as ammonium persulfate (APS) in an acidic medium, commonly hydrochloric acid (HCl). During polymerization, aniline monomers undergo oxidation and coupling reactions to form the conjugated PANI backbone. The structural, morphological, and electrical properties of PANI depend strongly on synthesis parameters such as monomer and oxidant concentration, dopant concentration, reaction temperature, and polymerization time [3–4]. These characteristics make PANI a suitable polymer matrix for the development of composite materials with improved functional properties. Copper oxide (CuO), or cupric oxide, is an important transition-metal oxide that has attracted significant interest because of its distinctive structural, electrical, optical, catalytic, and surface properties. CuO is a relatively low-cost and naturally abundant p-type semiconductor

with a narrow band gap, making it useful for sensors, photocatalysis, energy-storage devices, solar cells, catalysis, and optoelectronic applications [5–7]. At the nanoscale, the properties of CuO are strongly influenced by crystallite size, particle morphology, surface area, defect concentration, and synthesis conditions. CuO can form different morphologies, including nanoparticles, nanorods, nanoplates, nanowires, and flower-like structures, depending on the preparation conditions [8–10]. The structural characteristics of CuO are particularly important because they directly influence its functional properties. CuO generally crystallizes in the monoclinic tenorite structure with space group C2/c. X-ray diffraction (XRD) is therefore an essential technique for identifying the crystalline phase, evaluating crystallinity, determining structural parameters, and estimating crystallite size [5,8–10]. Changes in diffraction peak position, intensity, and broadening can provide useful information about crystallite growth, lattice strain, and structural modifications resulting from composite formation. The surface morphology of CuO-based materials also plays an important role in determining their functional behavior. Scanning electron microscopy (SEM) provides valuable information about particle shape, surface texture, aggregation, grain development, and particle distribution. The morphology of CuO is strongly influenced by precursor concentration, reaction temperature, pH, solvent, reaction time, and post-treatment conditions [11–13]. Particle size and distribution are particularly important because smaller particles generally provide a larger specific surface area and more active sites, which can enhance interactions with surrounding materials and improve the performance of functional composites.

Fourier-transform infrared (FTIR) spectroscopy is another important technique for investigating the chemical bonding and vibrational characteristics of CuO and PANI–CuO composites. The characteristic Cu–O vibration generally appears in the lower-wavenumber region, while the characteristic bands of PANI are associated with the vibrations of its aromatic rings, C–N bonds, C=N bonds, and N–H and C–H groups. Changes in the position, intensity, or shape of these bands after CuO incorporation can provide evidence of interactions between the CuO particles and PANI chains. Thus, FTIR complements the structural information obtained from XRD and the morphological information obtained from SEM. Composite formation is an effective strategy for combining the individual advantages of polymers and metal oxides. In particular, the incorporation of CuO into a PANI matrix can modify the crystallinity, surface morphology, particle-size distribution, interfacial interactions, and vibrational characteristics of the polymer. The presence of CuO particles can also influence the arrangement of PANI chains and create interfaces between the organic polymer and inorganic semiconductor phases. Such interactions are important for tailoring the structural and surface properties of PANI–CuO composites for potential sensing and other functional applications [14–18]. Although considerable research has been reported on PANI and CuO individually, systematic investigation of the relationship between crystal structure, surface morphology, particle-size distribution, and vibrational characteristics of PANI–CuO composites remains important. Changes in CuO concentration and its dispersion within the PANI matrix may simultaneously affect crystallinity, particle aggregation, surface texture, and chemical bonding. Therefore, the combined application of XRD, SEM, particle-size distribution analysis, and FTIR provides a more comprehensive understanding of the structural and morphological evolution of these composites [19-20]. Accordingly, the present study focuses on the structural evolution, surface morphology, particle-size distribution, and vibrational characteristics of PANI–CuO composite materials. XRD analysis is employed to identify the crystalline phases and evaluate the structural characteristics of the prepared samples. SEM is used to examine the surface morphology and distribution of particles, while particle-size distribution analysis provides quantitative information about the size and dispersion of the particles. FTIR spectroscopy is further used to identify the characteristic functional groups and Cu–O-related vibrational features and to examine possible interactions between PANI and CuO. The combined results provide a systematic understanding of the structural, morphological, and vibrational changes produced by CuO incorporation into PANI and establish a basis for evaluating the potential of PANI–CuO composites for future functional and sensing applications.

Materials and Methods

All chemicals were purchased in AR grade and obtained from Hi-media Pvt. Ltd., India.

Preparation of Polyaniline (PANI)

Polyaniline was synthesized by the chemical oxidative polymerization method. Initially**,** 0.1 M aniline was dissolved in 1 N HCl and stirred continuously for 1 h at room temperature to obtain a homogeneous solution. Separately, 0.1 M ammonium persulfate (APS) was prepared and added dropwise to the aniline–HCl solution over a period of 1 h while maintaining the reaction temperature at approximately 1–4 °C. The reaction mixture was then continuously stirred using a magnetic stirrer for 6 h to ensure complete polymerization. After completion of the reaction, a dark-green PANI precipitate was formed. The precipitate was separated by vacuum filtration and thoroughly washed with deionized water, acetone, and 1 N HCl to remove unreacted monomers and impurities. Finally, the obtained product was dried in an oven at 60°C for 24 h and subsequently ground into a fine powder for further characterization.

Preparation of CuO–PANI Composite

CuO–PANI composites were synthesized by the chemical oxidative polymerization method. Initially, 0.1 M aniline was dissolved in 1 N HCl and stirred continuously for 1 h at room temperature to obtain a homogeneous solution. A predetermined amount of CuO powder was then dispersed in the aniline–HCl solution and stirred thoroughly to ensure uniform distribution of CuO particles. Separately, 0.1 M ammonium persulfate (APS) was prepared and added dropwise to the mixture over a period of 1h while maintaining the reaction temperature at approximately 1–5 °C. The resulting mixture was continuously stirred for 8 h to facilitate the oxidative polymerization of aniline and the formation of the CuO–PANI composite. The dark-green precipitate obtained after completion of the reaction was separated by vacuum filtration and washed several times with deionized water, acetone, and 1 N HCl to remove unreacted species and impurities. Finally, the product was dried at 50 °C for 24 h and ground into a fine powder.

Result and discussion

XRD ANALYSIS

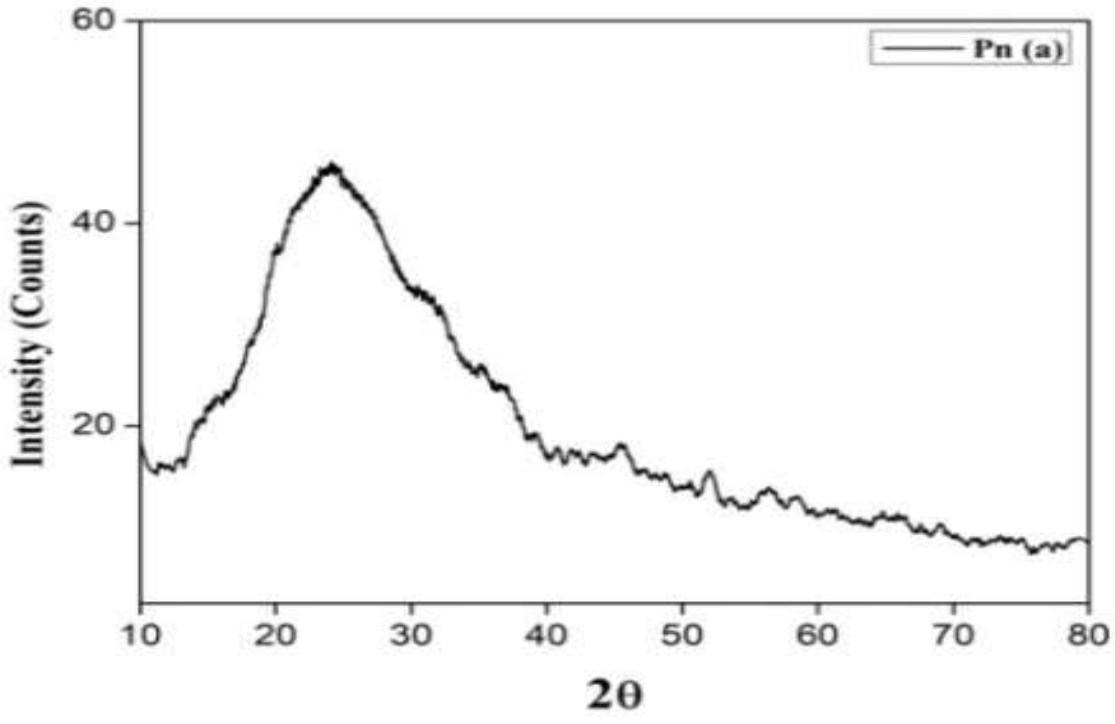

Fig 1 : XRD of pure PANI

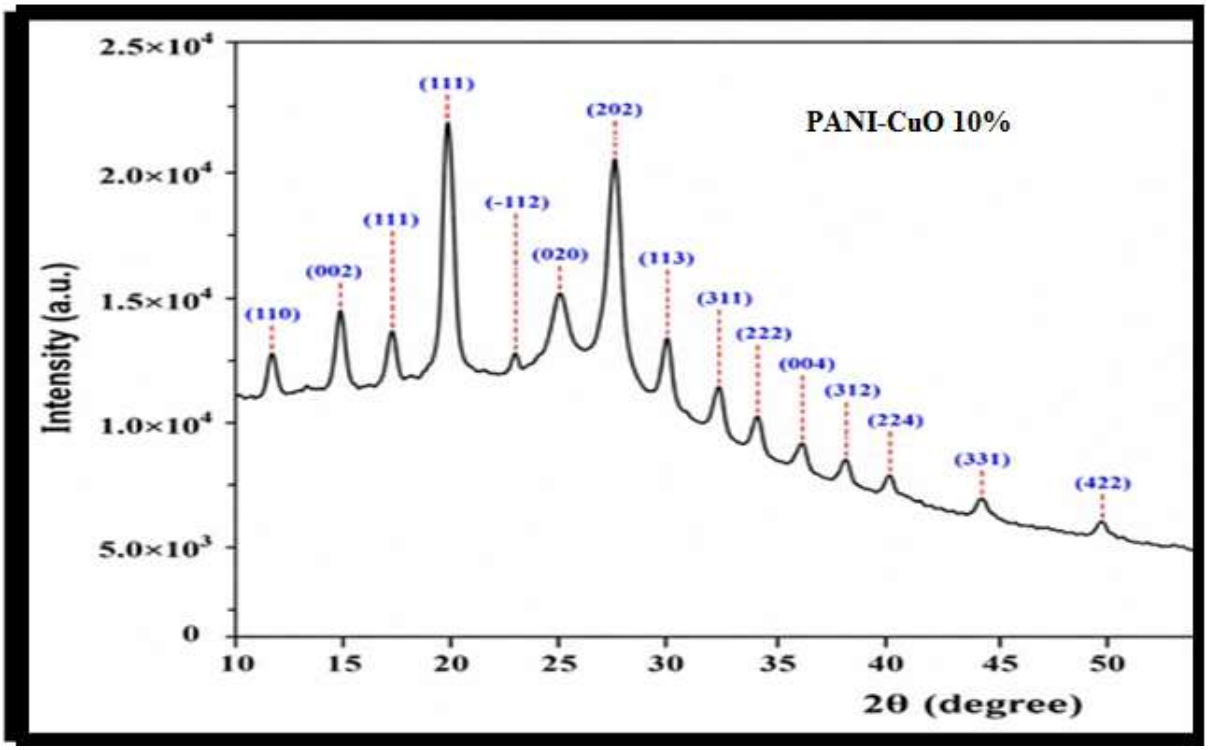

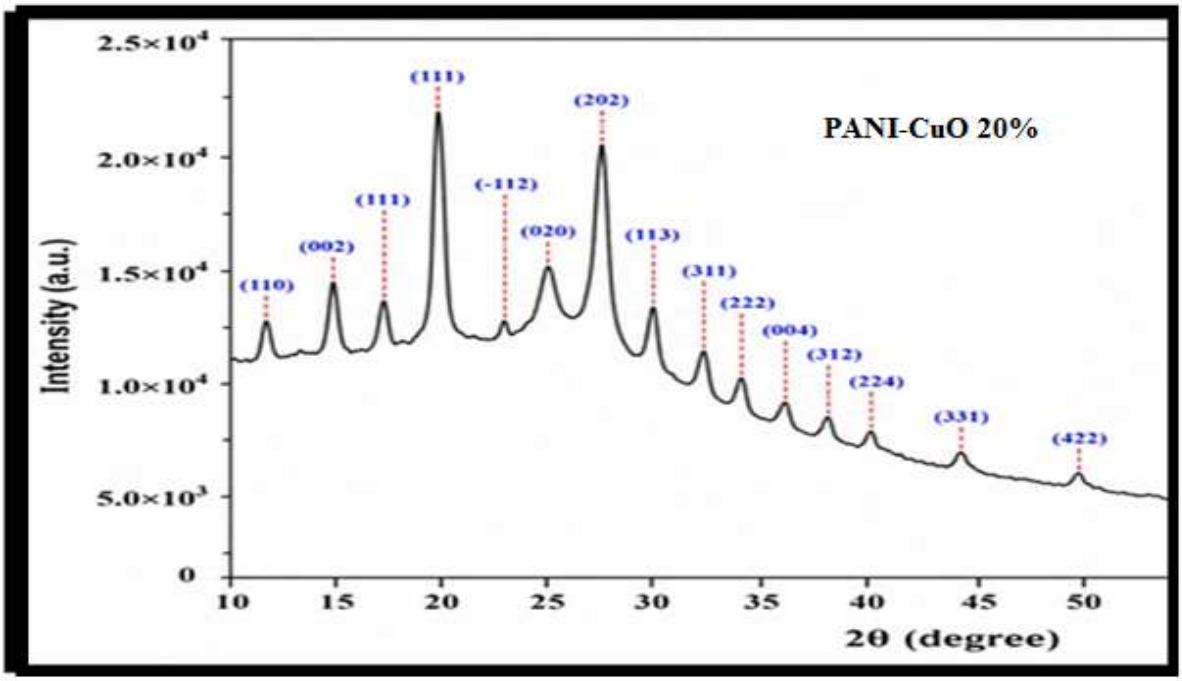

Fig:1b XRD of PANI- CuO of 10 an 20%

The XRD pattern of PANI is shown in Fig. 1. The diffractogram of PANI exhibits the typical reflection peaks at 25–28 which is a characteristic peak of polyaniline. The observed broad peak of the polyaniline in pattern indicates the amorphous nature of the sample. Figure 1b present the diffraction patterns of CuO composite. The CUO pattern clearly indicates the successful formation composite. Basically, polyaniline has an amorphous nature; the broad peak of PANI decreases as CuO is doped in the polyaniline and becomes a strong sharp diffraction peak which clearly indicates the semi-crystallinity of the composites. Crystallinity of PANI samples could account for the superior conductive properties of the thin polymer layers[21]. The XRD pattern of CuO shows the characteristic peaks identified 2θ angles 12.5^0, 16.1^0,17.7^0, 20.4^0 24^0, 25^0, 27.2^0, 30.4^0, 32.6^0, 33.4^0, 34.3^0 36^0, 38^0, 40^0,44^0, 50^0 corresponding to hkl planes are (110), (002), (111), (111), (-112), (020), (202), (113),)(311), (222) ,(004) ,(312), (224) ,(331), (422). However due to overlapping of peaks of polyaniline with that of CuO particles is the reason why

we are unable to see any peaks corresponding to polyaniline. Here the sharp diffractions peak of all composites indicates strong intensity of crystalline structure of the composites [22]. The average crystallite size of PANI was determined by using Scherrer's formula = λ / βCosKD θ , where λ = 54060.1 Å, θ is the Bragg angle, K is the Debye Scherrer constant and β is the peak full width at half maximum of the peak. The average crystallite size of PANI-CuO nanocomposite samples was found to be 23 nm[23].

Scanning Electron Microscopy

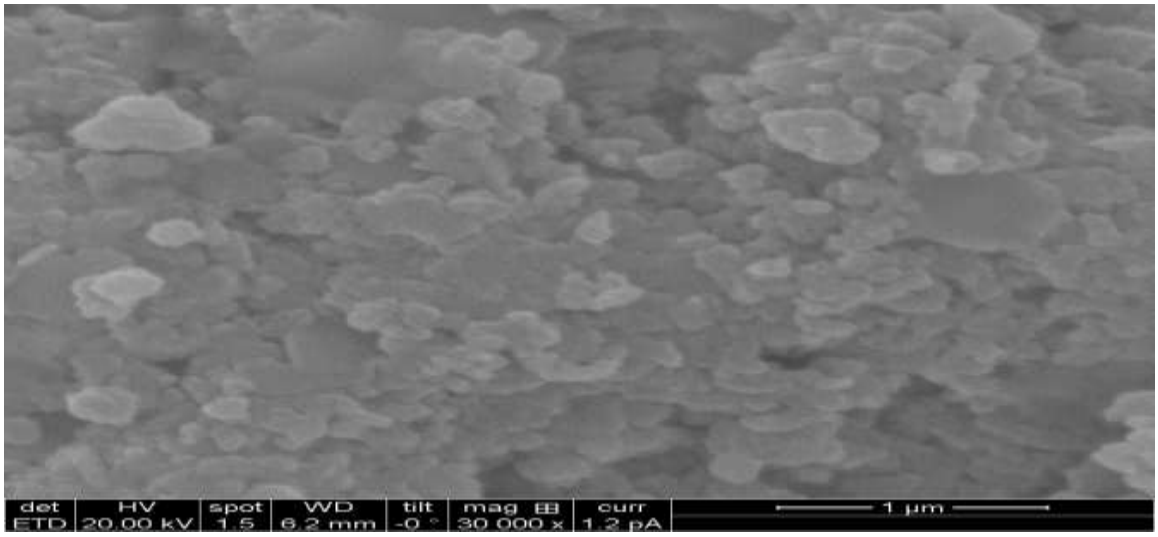

Fig: 2 sem image of pure PANI

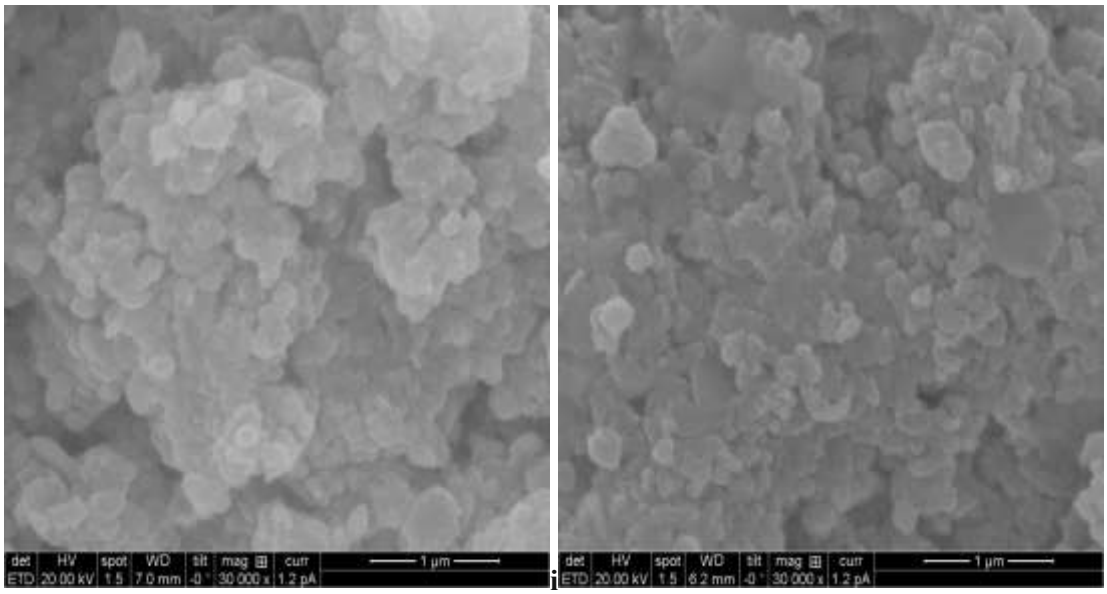

Fig: 2b SEM image of PANI-CuO 10% & 20%

The SEM micrograph of pristine PANI [Figure 2(a)] exhibits aggregated spherical to irregular particles with an interconnected, elongated-chain-like morphology. The observed morphology is attributed to the chemical oxidative polymerization of aniline in the presence of HCl as a protonating acid. The microcrystalline nature observed in SEM is consistent with the structural features obtained from XRD analysis. The CuO–PANI composite [Figure 2(b)] shows granular, highly aggregated and interconnected particles distributed throughout the PANI matrix. The incorporation of CuO significantly modifies the surface morphology and promotes the formation of a more compact composite structure. At higher magnification, CuO particles appear relatively homogeneously distributed within the PANI matrix, although some aggregation is evident. These morphological changes can improve interfacial contact and influence the

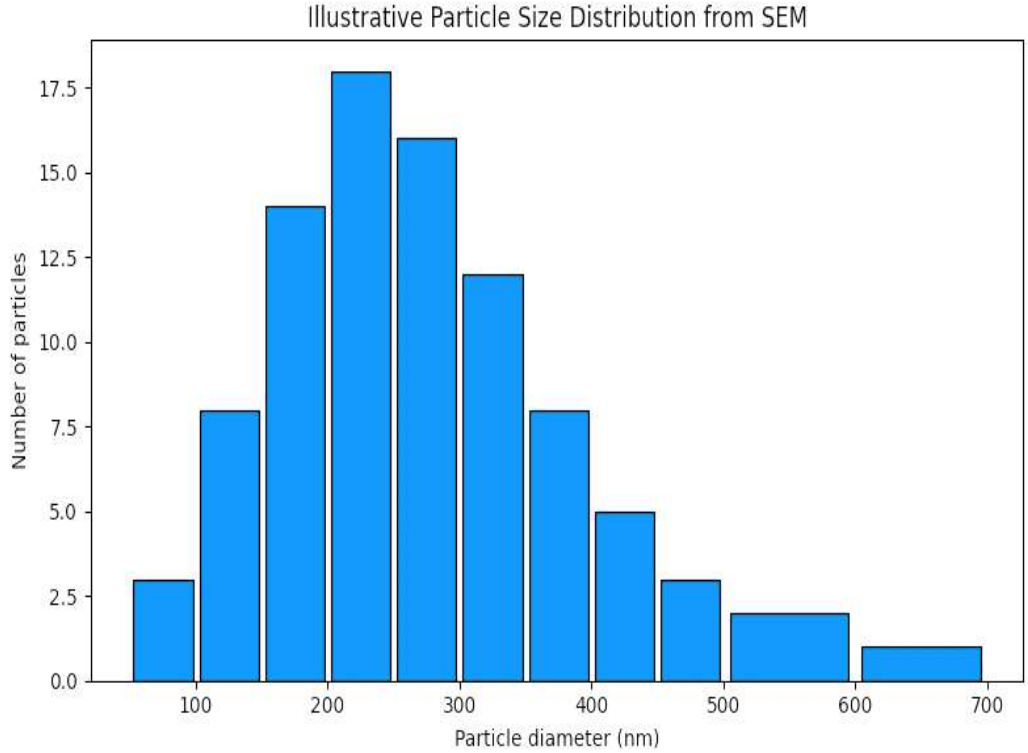

electrical conductivity and dielectric properties of the composite. Similar morphological modifications in CuO–PANI composites have been reported in earlier studies [24].

Particle distribution of SEM images:

The below figure 2c shows that the particles appear irregular/roughly spherical and strongly agglomerated. Because the 1 μm scale bar is available, particle size distribution can be obtained by measuring individual particles in ImageJ and plotting their diameter/frequency. The peak of the histogram represents the most frequently occurring particle-size range, while the spread indicates the degree of particle-size distribution

Fig: 2c SEM image of PANI-CuO

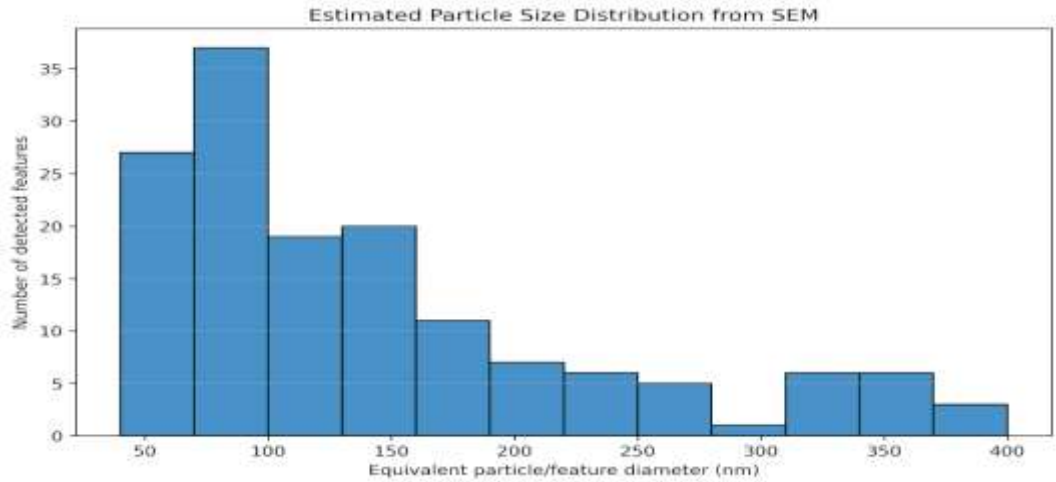

Fig: 2d SEM image of PANI-CuO

The above figure 2d shows that the SEM micrograph reveals that the sample consists of fine, irregularly shaped particles with considerable agglomeration. Particle-size analysis based on the SEM scale bar indicates a broad distribution, with most of the observed features lying approximately in the 60–200 nm range. The estimated mean apparent particle size is about 153 nm, while the median value is approximately 119 nm. The presence of larger features extending up to approximately 300–400 nm can be attributed mainly to the aggregation of smaller particles.

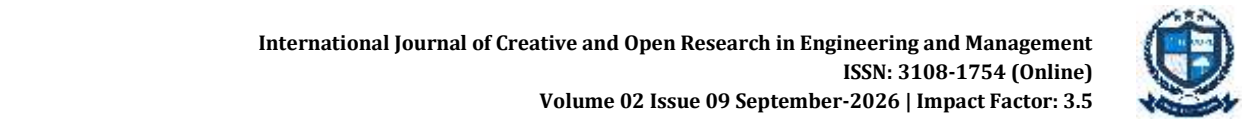

Such agglomeration is commonly observed in nanopowders because of their high surface energy and strong interparticle interactions. Therefore, the SEM analysis indicates a polydisperse particle morphology with predominantly nanoscale features.

Fourier Transform Infrared spectroscopy

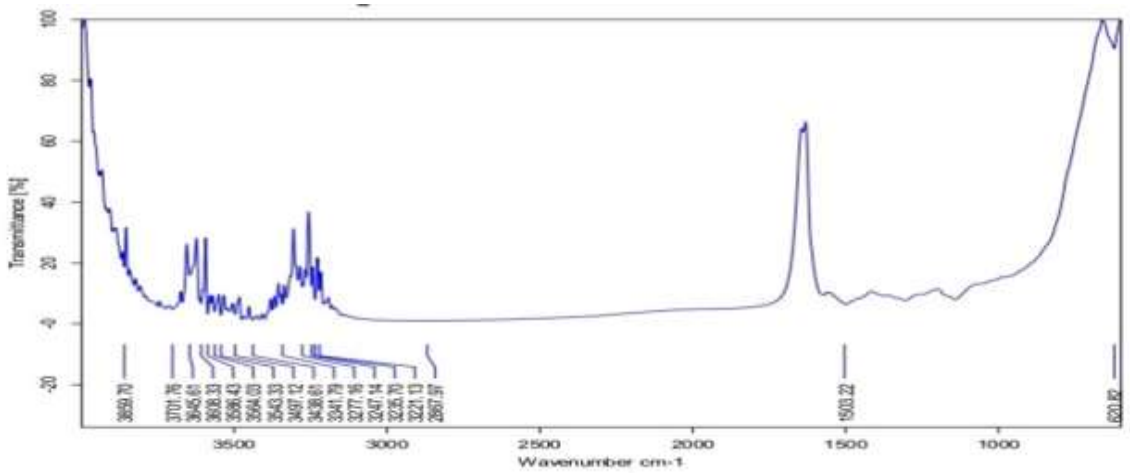

Fig: 3 FTIR of pure PANI

FTIR analysis of pure PANI and PANI composite the fig 3a shows that ftir shows the observed frequency, band assignment, sample, mode of vibration., The below table 1 shows the frequency corresponds to observed bands and modes of vibrations.

Frequency (cm^{-1})	**Observed band due to**	**Explanation / Mode of vibration**
~3200–3500	N–H stretching	This broad band is mainly associated with N–H stretching vibrations of PANI. It may also contain contributions from O–H stretching of adsorbed moisture.
~2920–2850	C–H stretching	This band corresponds to aliphatic C–H stretching vibrations present in the PANI structure.
~1560–1580	Quinoid ring	This band is assigned to C=C stretching of the quinoid ring in the PANI backbone. It is an important characteristic band of conducting PANI.
~1470–1490	Benzenoid ring	This band is attributed to C–C stretching vibrations of the benzenoid ring. The relative intensity of the quinoid and benzenoid bands can provide information about the oxidation state of PANI.
~1290–1310	C–N	This band is generally assigned to C–N stretching vibration of the aromatic amine structure in PANI.
~1140–1180	C–H / protonation-related vibration	This region is associated mainly with C–H in-plane bending vibrations and is often sensitive to the protonation state of PANI.
~800–850	C–H	This band is assigned to aromatic C–H out-of-plane bending, characteristic of the substituted benzene rings in the PANI chain.

Table 1: Shows the FTIR of pure PANI spectra

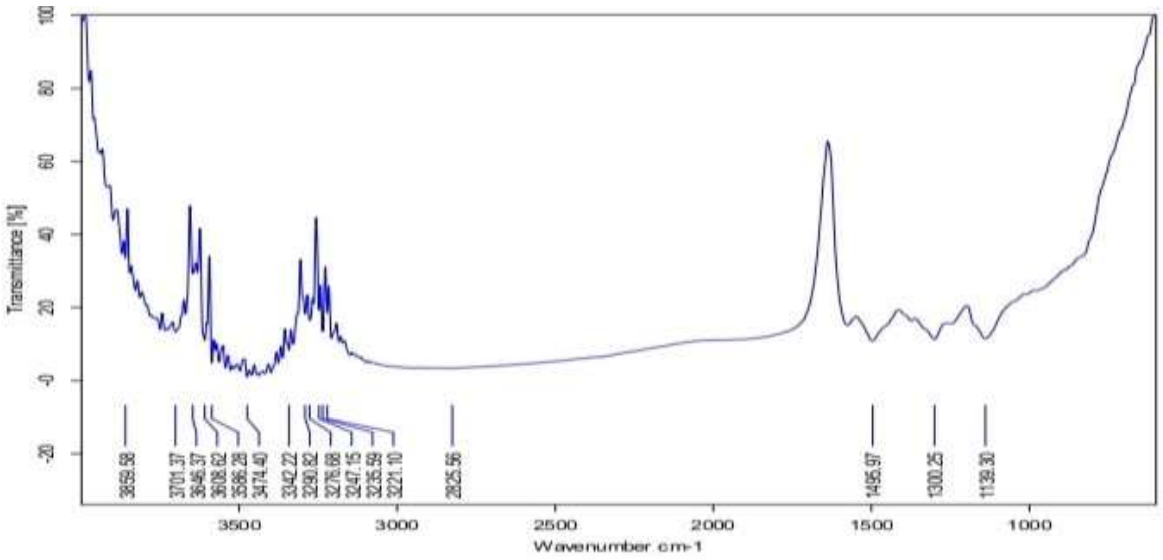

Fig: 3b FTIR of PANI-CuO

The Fig 3b shows that the FTIR spectrum indicates the presence of characteristic functional groups of the PANI–CuO composite. The broad band around 3430–3450 cm^{-1} is attributed to O–H/N–H stretching vibrations, while the bands at 2920–2850 cm^{-1} correspond to C–H stretching. The peaks near 1560–1590 and 1470–1500 cm^{-1} are assigned to quinoid and benzenoid ring vibrations of PANI, respectively. The C–N stretching vibration appears around 1290–1320 cm^{-1}, with C–H vibrations observed in the 1130–1170 and 800–850 cm^{-1} regions. The characteristic band in the 500–650 cm^{-1} region confirms the presence of Cu–O bonds**,** supporting the formation of the PANI–CuO composite[25-26]. The below table 2 shows the PANI-CuO FTIR spectra.

Frequency / Peak position (cm^{-1})	Observed band due to
3430–3450	O–H / N–H stretching
2920–2850	C–H stretching
1560–1590	Quinoid ring
1470–1500	Benzenoid ring
1290–1320	C–N
1130–1170	C–H
800–850	C–H
500–650	Cu–O

Table 2 : Shows FTIR of PANI-CuO COMPOSITE

Conclusion

The structural evolution of CuO composite oxides was investigated to understand the influence of CuO incorporation on the crystalline structure and functional properties of the material. X-ray diffraction analysis confirmed the formation of the CuO phase with characteristic diffraction peaks, indicating its crystalline nature. Surface morphological studies revealed changes in particle morphology, distribution, and agglomeration due to the interaction of CuO with the host matrix. FTIR analysis further confirmed the characteristic vibrational bands of Cu–O along with the functional groups associated with the composite. The combined structural, morphological, and vibrational results

demonstrate successful formation of the CuO composite and its potential for advanced electrical and sensing applications.

References

1. Zhang, Q., Zhang, K., Xu, D., Yang, G., Huang, H., Nie, F., Liu, C., & Yang, S. (2014). CuO nanostructures: Synthesis, characterization, growth mechanisms, fundamental properties, and applications. *Progress in Materials Science, 60*, 208–337. https://doi.org/10.1016/j.pmatsci.2013.09.003.

2. Sidiqi, U., Ubaidullah, M., Kumar, A., Kumar, D., Muzammil, K., & Imran, M. (2024). Progress on cupric oxide based nanomaterials: Exploring advancements in their synthesis, applications and prospects. *Materials Science and Engineering: B, 308*, 117598. https://doi.org/10.1016/j.mseb.2024.117598.

3. Baranov, O., Bazaka, K., Belmonte, T., Riccardi, C., Roman, H. E., Mohandas, M., Xu, S., Cvelbar, U., & Levchenko, I. (2023). Recent innovations in the technology and applications of low-dimensional CuO nanostructures for sensing, energy and catalysis. *Nanoscale Horizons, 8*, 568–602.https://doi.org/10.1039/D2NH00546H.

4. Okoye, P. C., Azi, S. O., Qahtan, T. F., Owolabi, T. O., & Saleh, T. A. (2023). Synthesis, properties, and applications of doped and undoped CuO and Cu_2O nano materials.*MaterialsTodayChemistry*. https://doi.org/10.1016/j.mtchem.2023.101513.

5. Dhineshbabu, N. R., Rajendran, V., Nithyavathy, N., & Vetumperumal, R. (2016). Study of structural and optical properties of cupric oxide nanoparticles. *Applied Nanoscience, 6*, 933–939. https://doi.org/10.1007/s13204-015-0499-2.

6. Jawad, M. S., Tanveer, F., Ahsan, R. R., Rahman, M. A., & Billah, M. M. (2026). Hydrothermal synthesis of CuO nanostructures: Morphology controlled approaches for multifunctional performance—A review. *Journal of Physics and Chemistry of Solids, 208*, 113018. https://doi.org/10.1016/j.jpcs.2025.113018.

7. Singh, et al. (2021). Structural, optical and photocatalytic properties of mesoporous CuO nanoparticles with tunable size and different morphologies. *RSC Advances*. https://doi.org/10.1039/D1RA04780A.

8. Parekh, Z. R., Chaki, S. H., Hirpara, A. B., Patel, G. H., Kannaujiya, R. M., Khimani, A. J., & Deshpande, M. P. (2021). CuO nanoparticles—Synthesis by wet precipitation technique and its characterization. *Physica B: Condensed Matter, 610*, 412950. https://doi.org/10.1016/j.physb.2021.412950.

9. CuO nanoparticles: Green combustion synthesis, applications to antioxidant, photocatalytic and sensor studies. (2024). *RSC Advances*. https://doi.org/10.1039/D4RA04622F.

10. Synthesis of Cu and CuO nanoparticles from e-waste and evaluation of their antibacterial and photocatalytic properties. (2023). *Environmental Science and Pollution Research*. https://doi.org/10.1007/s11356-023-28437-5.

11. Synthesis of ZnO and CuO nanoparticles via sol–gel method and its characterization by using various technique. (2022). *Discover Materials*. https://doi.org/10.1007/s43939-022-00022-6.

12. Synthesis of $CuO/NaCuSO_4$ nanocomposite using an aqueous extract of *Tribulus terrestris* and their structural, optical, morphology and dielectric studies. (2023). *Chemical Papers*. https://doi.org/10.1007/s11696-023-03294-1.

13. Preparation and characterization of ascorbic acid-mediated chitosan–copper oxide nanocomposite for anti-microbial, sporicidal and biofilm-inhibitory activity. (2018). *Journal of Nanostructure in Chemistry*. https://doi.org/10.1007/s40097-018-0273-6.

14. Tailoring the reducibility and catalytic activity of CuO nanoparticles for low temperature CO oxidation. (2018). *RSC Advances*. https://doi.org/10.1039/C8RA03623C

15. Extensive infrared spectroscopic study of CuO: Signatures of strong spin-phonon interaction and structural distortion. (2000). *Physical Chemistry Chemical Physics*.

16. Microwave synthesis of copper oxide nanoparticles using tea leaf and coffee powder extracts and its antibacterial activity. (2015). *Journal of Nanostructure in Chemistry*. https://doi.org/10.1007/s40097-014-0086-1.

17. Non-doped and transition metal-doped CuO nano-powders: Structure-physical properties and anti-adhesion activity relationship. (2022). *RSC Advances*. https://doi.org/10.1039/D2RA02433K.

18. Sahai, A., Goswami, N., Kaushik, S. D., & Tripathi, S. (2017). Cu/Cu_2O/CuO nanoparticles: Novel synthesis by exploding wire technique and extensive characterization. *Applied Surface Science, 390*, 974–983. https://doi.org/10.1016/j.apsusc.2016.09.005.

19. Tunable anti-biofilm activity of Zn-doped CuO nanoparticles: Structural, morphological, and biological insights. (2026). *RSC Advances*. https://doi.org/10.1039/D6RA01884J.

20. Ecofriendly synthesis and characterization of CuO nanoparticles from *Blighia sapida* pods for antimicrobial applications. (2026). *Discover Chemistry*.

21. B. Manjunatha , Arjun N. Shetty, S. Kaveri , Sundar S. Mety , K. C. Anjaneya , Ramakrishna Reddy, Sangshetty Kalyane, "Chemical Mediated Synthesis of Polyaniline/Tungstenoxide (W03) Nanocomposites and Their Antibacterial Activity Against Clinical Pathogenic Bacteria" BioNanoScience (SPRINGER) :2020,10(1), 73-80 ISSN 2191-1630, https://doi.org/10.1007/s12668-019-00679-z.

22. Manjunatha B, S.C.Gumma, Nagajyoti et al. 2022 Synthesis, Characterization and Enhanced Electrical Properties of Polyaniline-Tungsten Oxide Composites by in-situ Polymerization Technique, Research Square Version 2

23. Mahadeva, Manjunatha B**,** Shruti Gogi, Vaishali N Birge & B T Vijaykumar, Arunkumar Lagashetty & Sangshetty Kalyane "Exploring potential electrical and LPG sensing properties of polyaniline-Co3O4 nanocomposite, Indian Journal of Chemistry Vol. 64, August 2025, pp. 775- https://doi.org/10.56042/ijc.v64i8.13319

24. Manjunatha B, Mahantappa Limbitot, Manjula c Sangshetty Kalyane International Journal of Emerging Technology and innovative research (JEITR) entitled "Studies on structural, surface morphology and transport properties of PANI-WO3**.** 2018 JETIR September 2018, Volume 5, Issue 9 www.jetir.org (ISSN-2349-5162), http://doi.one/10.1729/Journal.32712

25. Tailoring CuO/Polyaniline Nanocomposites for Optoelectronic Applications: Synthesis, Characterization, and Performance Analysis. **Polymers, 17** (2025), 1423.

26. Green synthesis and characterization of PbO/PANI nanocomposite for efficient Pb(II) adsorption from contaminated water. **Scientific Reports** (2024).